

Specialty fibers for high power lasers and amplifiers

Jayanta K. Sahu, Deepak Jain, and Yongmin Jung

Optoelectronic Research Center, University of Southampton, Southampton SO17 1BJ, UK

(INVITED PAPER)

ABSTRACT

This paper reviews our recent work on novel large-mode area fibers for high power lasers and amplifiers. An ultra-low-NA fiber and single-trench fiber have been proposed for mode area scaling of the fundamental mode. In case of single-trench fiber design, resonant coupling of the higher order modes has been exploited to achieve effective single mode operation in fiber with large effective mode area. Our proposed fiber designs are easy to fabricate using conventional low-loss fiber fabrication techniques, and moreover, being all solid structure, they ensure easy cleaving and splicing. A monolithic and compact high power fiber laser/amplifier device with a good output beam quality can be achieved using Single-trench fiber design.

1. INTRODUCTION

Fiber lasers, due to their excellent performance, have gained more and more attentions of industrial laser users and are currently being explored for a wide range of applications [1-2]. However, the output power level of fiber laser is challenged by the detrimental non-linear effects [3]. Large mode area (LMA) fiber designs can avoid non-linear effects by increasing their threshold. In addition, LMA fiber designs should also offer other features such as effective single mode operation to ensure good output beam quality, bend robustness, and easy cleaving and fusion splicing. Over the past few years, different LMA fiber designs have been proposed such as photonic crystal fiber (PCF) [4], leakage channel fiber (LCF) [5], Polygonal-chirally coupled core fibers (P-CCC) [6], and photonic bandgap based fibers such as 2D-all solid photonic bandgap fiber (2D-ASPBGF) [7] and Bragg fiber [8]. However, most of these designs do not offer delocalization of the higher order modes (HOMs) and mostly rely on loss of the HOMs. Moreover, they require complex fabrication procedures due to stringent requirement of same refractive index of core and cladding, and non-circular fiber symmetry. Recently we have demonstrated ultra-low-NA (~ 0.038) step index fibers (SIFs). Our ultra-low NA SIF can provide an effective area (A_{eff}) of $\sim 700\mu\text{m}^2$ at $\sim 32\text{cm}$ bend radius while following the criterion of the higher order mode loss to be higher than 10dB/m and the fundamental mode (FM) is lower than 0.1dB/m [9]. An ultra-low-NA rare-earth doped fiber of ~ 0.038 (corresponding to core refractive index of 0.0005 with respect to cladding) has been demonstrated, for the first time to the best of our knowledge, using solution doping technique in conjunction with modified chemical vapour deposition (MCVD) process [9]. Further a passive Ge-doped ring surrounding the fiber core has been used to filter out the HOMs. This design, known as single trench fiber (STF), enhances the suppression of the HOMs by increasing the losses of the HOMs and reducing their overlap with the core which further enhances the mode area scaling capability of FM [10-12]. A STF can offer an A_{eff} of $\sim 1,000\mu\text{m}^2$ at $\sim 40\text{cm}$ bend diameter, while offering the criterion of 10 dB/m loss for the HOMS and keeping the loss of the FM lower than 0.1 dB/m [10-12].

2. RA LOW NA STEP INDEX FIBERS

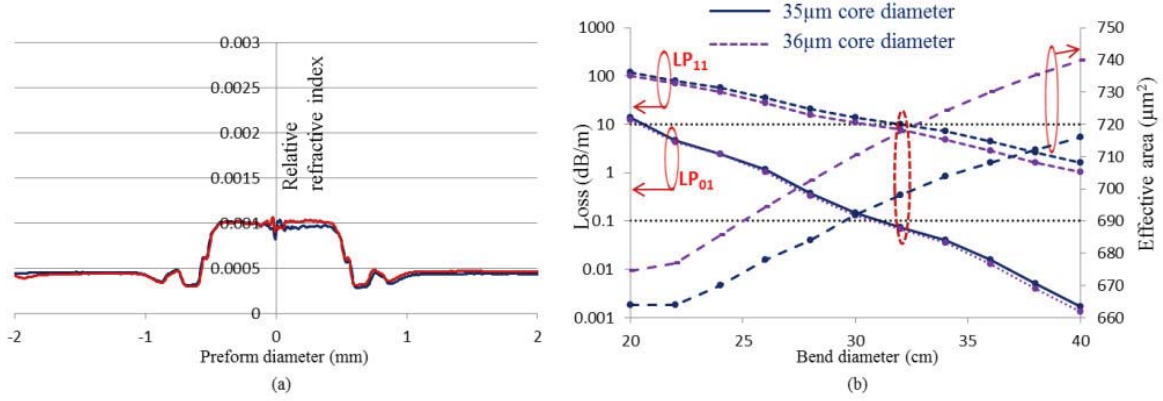


Fig. 1(a) Refractive index profile of fabricated low-NA Yb-doped step-index preform. (b) The calculated loss of LP_{01} and LP_{11} modes and effective area of the LP_{01} mode of a SIF w.r.t. bend diameters at wavelength of 1060nm and for two different core diameters. The core Δn is 0.0005 (corresponding NA of 0.038).

Fig. 1(a) shows the refractive index profile of an ultra-low NA of 0.038 (corresponding core refractive index with respect to the cladding as 0.0005) Yb-doped step-index preform fabricated using our optimized MCVD process in conjunction with solution doping process. The plot shows a flat profile without any considerable dip at the center of the core. Our fabrication process ensures good reproducibility and good yield as well. Effective-single mode operation is confirmed by ensuring HOMs losses larger than 10 dB/m while only 0.1dB/m loss for the FM as shown in Fig. 1(b). Numerical simulations show the feasibility of scaling the effective area of the FM to $700\mu\text{m}^2$ (taking bend induced distortion into account) at a bend diameter of 32cm for a SIF of 35 μm core diameter and 0.038 NA. On the other hand, for a core NA of 0.048, the maximum possible effective area is limited to $\sim 450\mu\text{m}^2$ for a core diameter of $\sim 29\mu\text{m}$ and at a bend diameter of $\sim 15.5\text{cm}$. Our analysis provides a strong motivation to fabricate ultra-low NA SIFs. In order to verify the effective-single-mode operation, we drew the fiber to a core diameter of 35 μm and outer diameter of 420 μm with low index coating. Before drawing the fiber, preform was milled to D-shape to increase the pump absorption. Fiber shows 2dB/m cladding absorption at $\sim 975\text{nm}$.

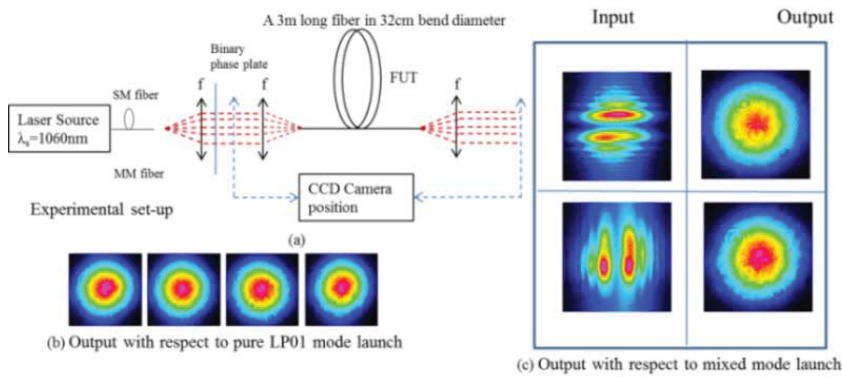


Fig. 2(a) Experimental set-up used for single mode verification (b) output beam profile with respect to LP_{01} mode launch and (c) output beam profile with respect to mixed mode launch. A 3m long fiber coiled at 32cm bend diameter was used in this experiment.

Fig. 2(a) shows the experimental set-up used for the verification of effective single mode operation at 1060nm. A 3m long fiber coiled at 32cm bend diameter is used as fiber under test (FUT). Fiber output ensures a Gaussian beam irrespective of the profiles of the launched input beams as shown in Fig. 2(b) and 2(c). Furthermore, the fiber was tested in a 4%-4% laser cavity. A laser diode operating at $\sim 975\text{nm}$ was used as a pump source. A 7m long fiber coiled at 32cm

bend diameter was used for this experiment. A maximum output power of ~50W was obtained at ~72W of launched pump power as shown in Fig. 3(a). The output power is limited by the available pump power. A slope efficiency of ~81% was measured with respect to the absorbed pump power and a M^2 of ~ 1.1. The output spectrum (Fig. 3(b)) shows the free running laser operating at 1040nm.

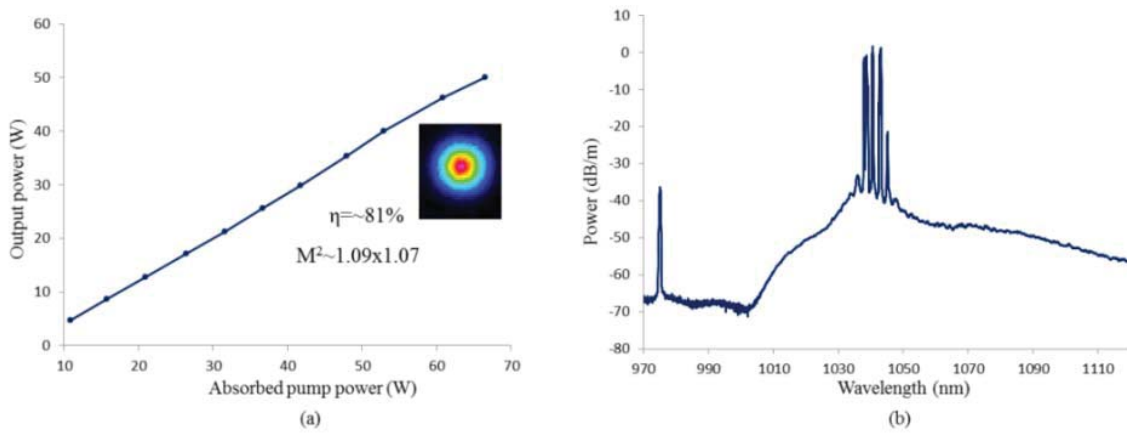


Fig. 3(a) Slope efficiency of a 7m long Yb-doped 0.038 NA SIF. Inset shows the profile of the output beam, (b) measured output spectrum taken at an OSA with a resolution of 0.2nm.

3. SINGLE TRENCH FIBERS

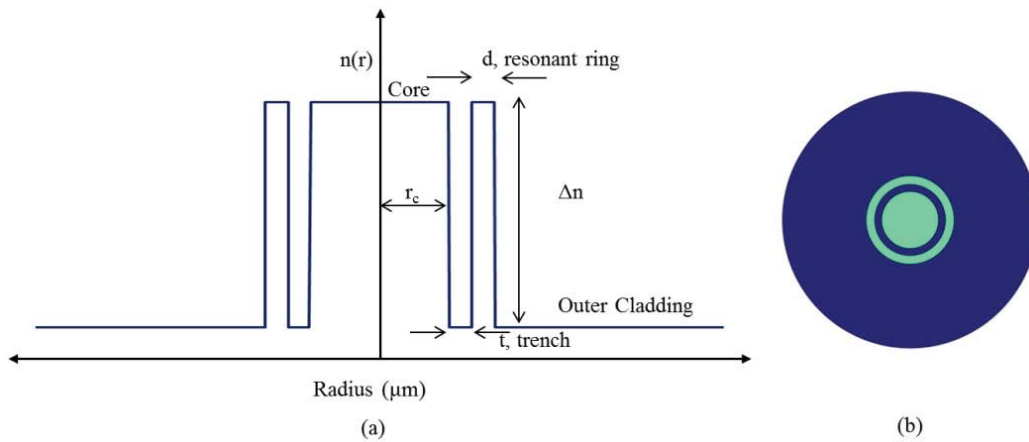


Fig. 4 (a) Schematic refractive index profile and (b) cross-section of the STF. Green and blue colours represent high and low-refractive index regions respectively.

Figure 4 shows the schematic of both refractive index profile and the 2D-cross section of our proposed STF design. Figure 5 shows the loss characteristics and power fraction in core for different modes, and the effective area of the FM of a $40\mu\text{m}$ STF for different thicknesses of trench and resonant ring. The core NA is fixed at ~0.038 and the bend radius at 20cm. The operating wavelength used in our simulation is 1060nm. Figure 5(a) shows the calculated loss of the FM and HOM having lowest loss among all the possible HOMs of the fiber. It includes, all HOMs of core, all modes of

resonant ring, mixed modes, and their polarizations. We have verified that for each resonant ring and trench thicknesses shown in Fig. 5(a), other possible HOMs (excluding FM and least lossy HOM as shown in Fig. 5(a)) in fiber have loss higher than 10dB/m. Figure 5(b) shows their corresponding power fraction in core and Fig. 5(c) shows the A_{eff} of the FM. For several combinations of thicknesses of the trenches and resonant rings, the loss of the FM remains lower than 0.1dB/m and power fraction in core is higher than 80% while the loss of the HOMs are higher than 10dB/m or have at least 30% lower power fraction in core compared to FM. The A_{eff} of the FM varies from $850\mu\text{m}^2$ to $1120\mu\text{m}^2$ depending on the resonant ring and trench thicknesses (including bend induced distortions at 20cm bend radius).

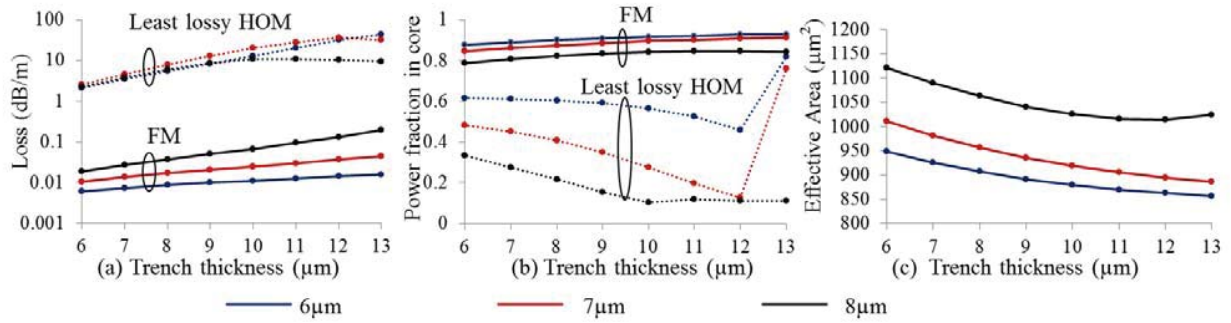


Fig. 5(a) Loss of the FM and the least lossy HOM and (b) Power fraction in core for FM and least lossy HOM, and (c) A_{eff} of the FM for different resonant ring and trench thicknesses for $40\mu\text{m}$ core STF with $\Delta n=0.0005$ at 20cm bend radius.

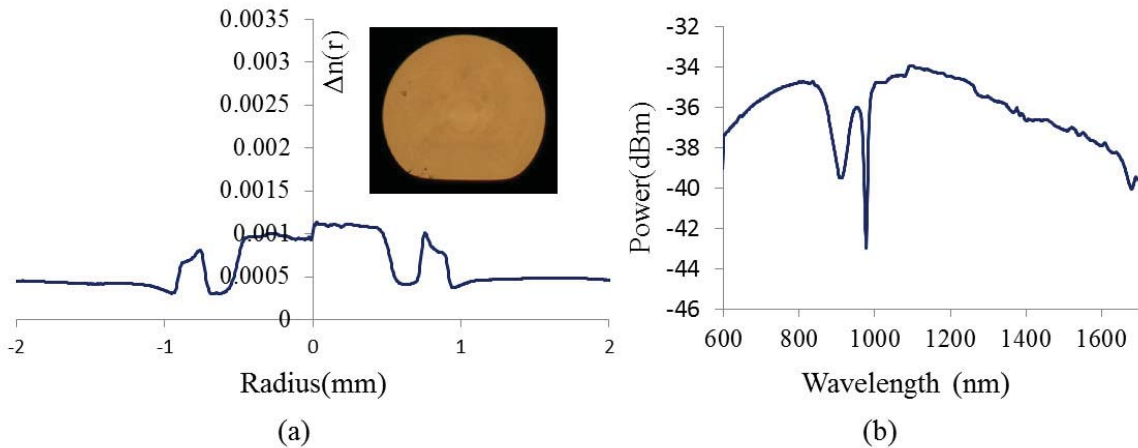


Fig. 6(a) RIP of Yb-doped alumino-silicate STF preform. Inset shows the microscope image of fiber end facet, and, (b) White light absorption spectrum of a 1.55m long fiber.

We fabricated a $40\mu\text{m}$ core STF preform using MCVD process in conjunction with solution doping technique. The core is Yb-doped alumino-silicate and the resonant ring Ge-doped silica. Fig. 6(a) shows the refractive RIP of fabricated preform having a NA of ~ 0.038 . The slight asymmetry in preform profile is a measurement artifact only. We obtained the flat index profile for core even for such a low NA using our optimized fabrication process over a preform length of $\sim 400\text{mm}$. The outer diameter of preform was 12mm, which was further etched down to 6mm using hydrofluoric acid. Etched preform was then milled to have a D-shape and subsequently drawn into a fiber with cladding diameter of $\sim 233\mu\text{m}$. The core diameter is $\sim 40\mu\text{m}$, trench thickness (t) is $\sim 9\mu\text{m}$, and resonant ring thickness (d) is $\sim 7\mu\text{m}$. The fiber was coated with a low-index polymer which provided a nominal pump cladding NA of 0.48. Inset of Fig. 6(a) shows the microscope image of fiber cross-section. Fig 6(b) shows the white light absorption spectrum of $\sim 1.55\text{m}$ long fiber and the absorption is 8dB/m at 976nm.

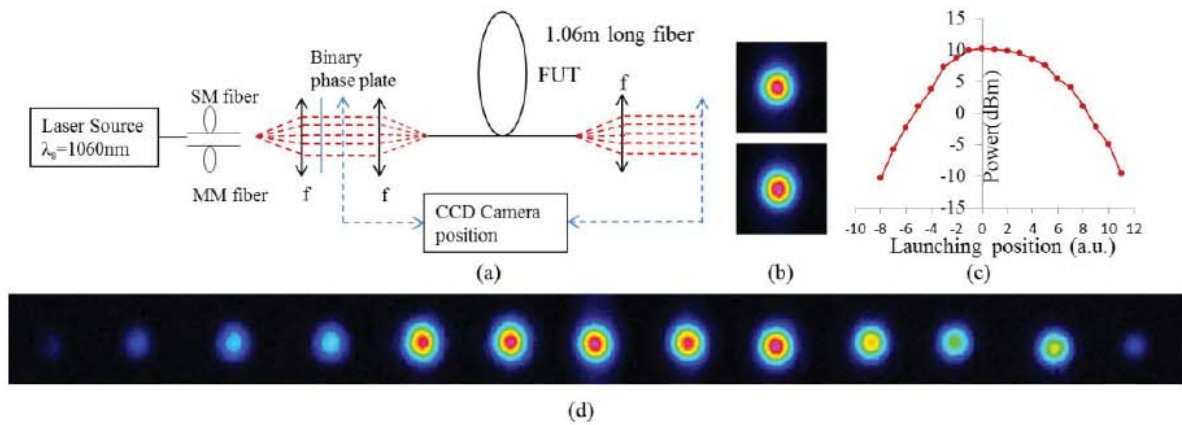


Fig. 7(a) Experiment set-up used for single-mode characterization of STF (b) output with respect to optimum launching of single mode in loosely coiled and bent at 20cm conditions (c) output power with respect to offset launching of single mode input (d) output beam profile with respect to offset launching of single mode input.

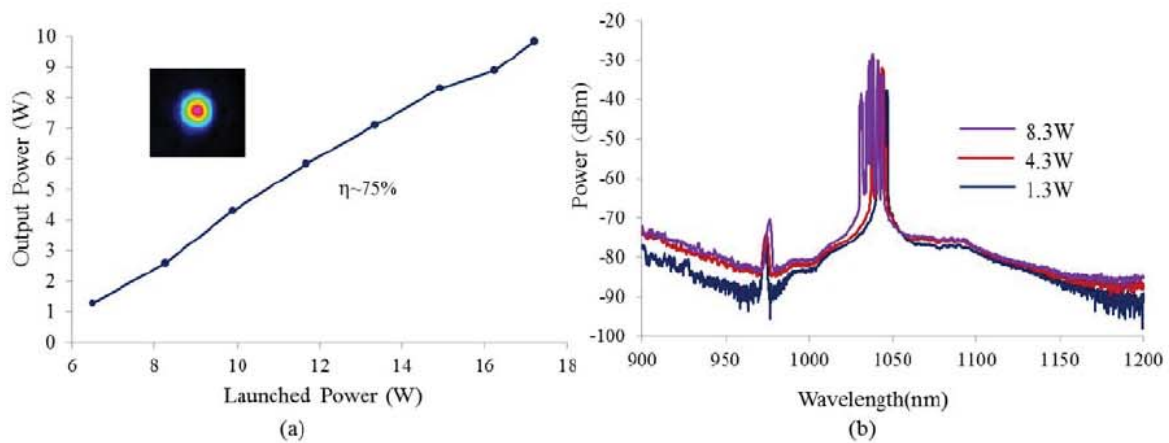


Fig. 8(a) Laser slope efficiency of a 3.3m long STF. Inset shows the profile of output beam (b) measured spectrum of output beam at different power levels.

Figure 7(a) shows the experiment set-up used for verification of single mode behavior of the fiber. Here we measured the output of FUT for different input launching conditions. The aim of different launching conditions is to increase the probability of HOMs excitation. A ~1m long fabricated STF was used as FUT. We stripped the polymer coating and applied high index oil at both ends to remove cladding modes. In order to facilitate the HOMs' excitation conditions by exploiting different modal field diameters (MFDs) and NAs of input beam and FUT, a single mode laser operating at 1060nm wavelength was launched into FUT using a single mode fiber spliced to beam delivery fiber of laser source. Figure 7(b) shows the obtained output beam under two conditions of FUT namely loosely coiled and bent at 20cm bend radius, which ensures a Gaussian output beam. In order to further enhance the multimode excitation, we use offset launching of input beam. Figure 7 (c-d) shows the measured power of output beam and output beam profiles for different offset launchings of input beam respectively. The power level of output beam with respect to misalignment of launching beam along x-axis follows a nearly Gaussian curve, on the other hand the output beams ensure a Gaussian beam output irrespective of launching conditions. It is interesting to observe from Fig. 7(d) that, only the intensity of the output beam changes but it remains Gaussian, which ensures high loss for the HOMs. To further validate the single mode behaviour of fiber, we launched multimode light into FUT by splicing the multimode optical fiber to the delivery fiber of 1060nm

laser source, as shown in Fig. 7 (a). Furthermore, a binary phase plate was used to launch LP_{11} and LP_{21} modes. The output profiles in all cases ensure high suppression of HOMs [12]. Figure 8(a) shows the laser output power with respect to launched pump power in a 4%-4% laser cavity, and we obtained a slope efficiency of $\sim 75\%$. Inset shows the output beam profile and a M^2 of ~ 1.15 was obtained. Figure 8(b) shows the OSA spectrum taken at different output power levels. The laser is operating at wavelengths around 1040nm.

4. CONCLUSION

We have demonstrated a novel single-trench optical fiber design for mode area scaling thanks to the ultra-low NA and resonant coupling of the higher order modes of core to the resonant ring surrounding the core. Our proposed fiber structure can be easily fabricated using conventional modified chemical vapour deposition (MCVD) technique in conjunction with solution doping process. Experimental results and simulations strongly indicate that single-trench fiber is a good candidate for power scaling of fiber lasers and amplifiers.

5. ACKNOWLEDGEMENT

The work is supported by the EPSRC Centre for the Innovative manufacturing in Photonics EP/HO2607X/1.

6. REFERENCES

- [1] Jauregui C., Limpert J., and Tunnermann A., "High-power fiber lasers," [Invited], *Nature Photonics* **7**, 861-867 (2013).
- [2] Zervas M. N. and C. A. Codemard, "High Power Fiber Lasers: A Review," [Invited], *IEEE JSTQE* **20**, 0904123 (2014).
- [3] Agrawal G. P., "Nonlinear Fiber Optics," 3rd ed. New York: Academic (2001).
- [4] Limpert J., Liem A., Reich M., Schreiber T., Nolte S., Zellmer H., and Tunnermann A., "Low-nonlinearity single-transverse-mode ytterbium-doped photonic crystal fiber amplifier," *Opt. Exp.* **12**, 1313-1319 (2004).
- [5] Gu G., Kong F., Hawkins T. W., Foy P., Wei K., Samson B., and Dong L., "Impact of fiber outer boundaries on leaky mode losses in leakage channel fibers," *Opt. Exp.* **21**, 24039-24048 (2013).
- [6] Ma X., Zhu C., I-Ning Hu, Kaplan A., and Galvanauskas A., "Single-mode chirally-coupled-core fibers with larger than 50 μm diameter cores," *Opt. Exp.* **22**, 9206-9219 (2014).
- [7] Gu G., Kong F., Hawkins T., Parsons J., Jones M., Dunn C., Kalichevsky-Dong M. T., Saitoh K., and Dong L., "Ytterbium-doped large-mode-area all-solid photonic bandgap fiber lasers" *Opt. Exp.* **22**, 13962-13968 (2014).
- [8] Dianov E. M., Likhachev M. E., and Fevrier S., "Solid-core photonic bandgap fibers for high-power fiber lasers," *IEEE J. Sel. Top. Quant. Electron.* **15**, 20-29 (2009).
- [9] Jain D., Jung Y., Barua P., and Sahu J. K. "Demonstration of ultra-low NA rare-earth doped step index fiber for applications in high power fiber lasers," *Opt. Exp.*, **23**, 7407-7415 (2015).
- [10] Jain D., Baskiotis C., Kim J., and Sahu J. K., "First demonstration of single trench fiber for delocalization of higher order modes," [Contributed upgraded to Invited] in *Conference on Lasers and Electro-Optics(CLEO)*, San Jose, Calif., 2014, paper SF1N.1.
- [11] Jain D., Baskiotis C., May-Smith T. C., Kim J., and Sahu J. K., "Large mode area multi-trench fiber with delocalization of higher order modes [Invited]," *IEEE JSTQE*, **20**, 0902909, (2014).
- [12] Jain D., Jung Y., Nunez-Velazquez M., and Sahu J. K. "Extending single mode performance of all-solid large-mode-area single trench fiber," *Opt. Exp.*, **22**, 31078-31091 (2014).